VLTI-AMBER observations of η Carinae with high spectral resolutions of 1,500 & 12,000

G. Weigelt[1], R. G. Petrov[2], O. Chesneau[2], K. Davidson[3], A. Domiciano de Souza[2], T. Driebe[1], R. Foy[4], D. Fraix-Burnet[5], T. Gull[6], J. D. Hillier[7], K.-H. Hofmann[1], S. Kraus[1], F. Malbet[5], A. Marconi[8], P. Mathias[2], J.-L. Monin[5], F. Millour[2], K. Ohnaka[1], F. Rantakyrö[9], A. Richichi[10], D. Schertl[1], M. Schöller[9], P. Stee[2], L. Testi[8], M. Wittkowski[9]

[1]MPI for Radioastronomy, [2]Univ. Nice, [3]Univ. Minnesota, [4]Univ. Lyon, [5]Univ. Grenoble, [6]GSFC, [7]Univ. Pittsburgh, [8]Univ. Firence, [9]ESO

Abstract: We present the first NIR spectro-interferometry of the LBV η Carinae (Weigelt et al. 2006). The observations were performed with the AMBER instrument of the ESO VLTI in Dec. 2004 and Feb. 2005. The aim of this work is to study the wavelength dependence of η Car' s optically thick wind region with a high spatial resolution of 5 mas (11 AU) and high spectral resolution. The observations were carried out with three 8.2 m Unit Telescopes in the K band. The raw data are spectrally dispersed interferograms obtained with spectral resolutions of 1,500 (MR-K mode) and 12,000 (HR-K; Fig. 1). The observations were performed in the wavelength range around both the He I 2.059 µm and the Br γ 2.166 µm emission lines. The spectrally dispersed interferograms allow the investigation of the wavelength dependence of the visibility, differential phase, and closure phase. If we fit Hillier et al. (2001) model visibilities to the observed AMBER visibilities, we obtain 50% encircled-energy diameters of 4.3, 6.5 and 9.6 mas in the 2.17 µm continuum, the He I, and the Br γ emission lines, respectively. The AMBER measurements are in good agreement with predictions of the radiative transfer model of Hillier et al. (2001). Our observations support theoretical models of anisotropic winds from fast-rotating, luminous hot stars with enhanced high-velocity mass loss near the polar regions.

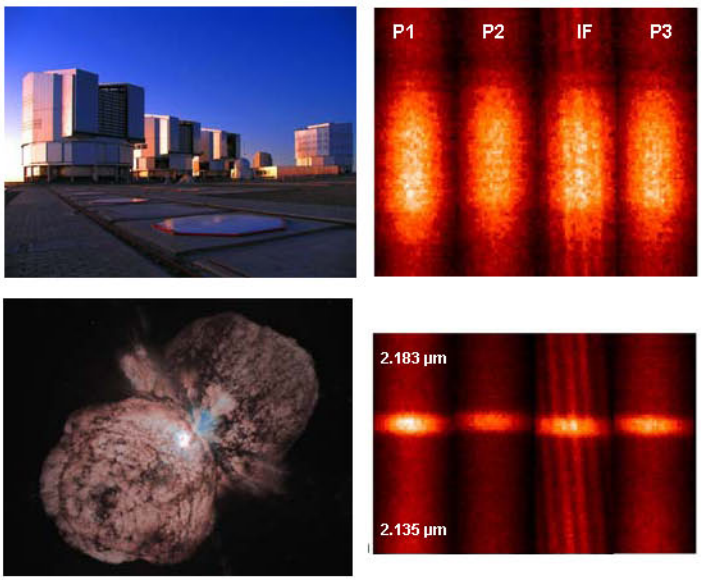

Fig. 1. Left: VLTI; η Car/Homunculus nebula (HST). Right: Spectrally dispersed VLTI/AMBER Michelson interferograms of η Car. The two panels show the spectrally dispersed fringe signal (IF) as well as the photometric calibration signals from the three telescopes (P1-P3) in high (HR, λ/Δλ = 12,000; upper panel) and medium spectral resolution mode (MR, λ/Δλ = 1,500; lower panel). In both panels, the bright regions are the Doppler-broadened Br γ emission line.

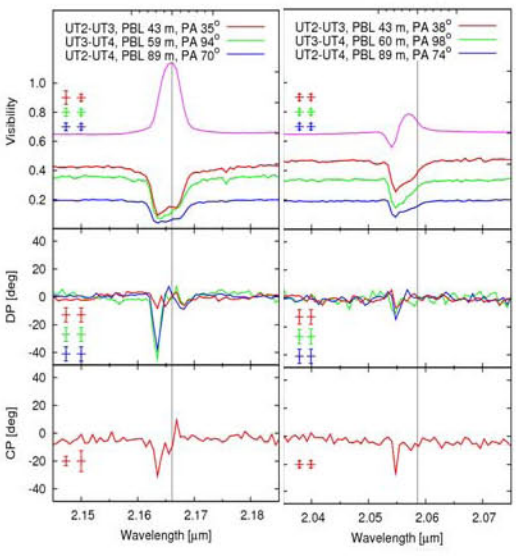

Fig. 2. AMBER observables derived from our η Car medium resolution data around the Br γ and He I line (spectral resolution 1,500; Dec. 2004). The pink curves (top) show the spectra, followed by the derived calibrated visibilities (red, green, blue). In the second and third row, the differential phase (DP) and the closure phase (CP) are presented. The vertical grey line marks the rest-wavelength of Br γ and He I (left error bar: continuum; right error bar: line).

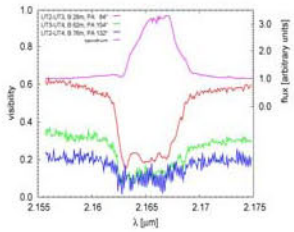

Fig. 3. Spectrum (pink) and calibrated η Car visibilities (red, gree, blue) derived from our AMBER data taken with high spectral resolution of λ/Δλ = 12,000 within the Br γ (Feb. 2005).

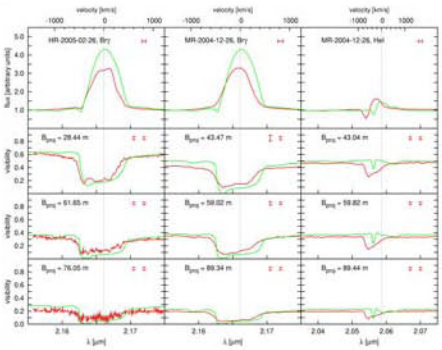

Fig. 4. Comparison of the AMBER spectra and visibilities with the model predictions of Hillier et al. (2001). The figure displays the spectra (upper row) and visibilities (lower three rows) of the four AMBER measurements (red) and the corresponding data of the Hillier et al. model (green). In the case of the He I line, the differences are larger, indicating a different physical process involved in the line formation (Nielsen et al. 2006, Hillier et al. 2006).

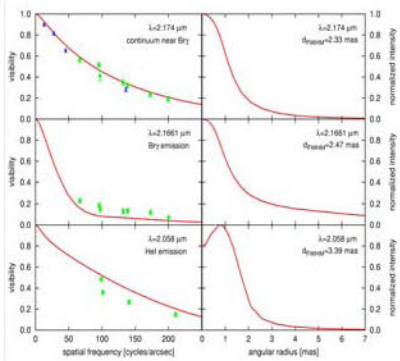

Fig. 5. Left: Comparison of the AMBER visibilities (filled green squares; baseline range 28-89 m) as a function of spatial frequency with the model predictions of Hillier et al. 2001 (red lines) for the continuum (upper panel), the central wavelength of the Br γ, and He I emission line (bottom). The blue triangles are the VINCI K-band measurements from van Boekel et al. (2003). Right: Center-to-limb variation of the monochromatic Hillier et al. (2001) models for the wavelengths indicated by the labels.

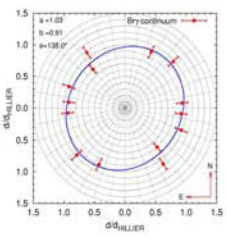

Fig. 6. Polar diagram showing 1-D diameter fits of the measurements as a function of position angle for the continuum region near the Br γ line. The 1-D diameters are the results from the fits of the model of Hillier et al. (2001) to the observed visibilities. The blue line represents the best ellipse fit of the diameters (the continuum Hillier diameter $d_{Hillier}$ corresponds to 2.33 mas FWHM).

Results: We resolved η Car' s optically thick wind region in the continuum and within the Br γ & He I line (Figs. 2 & 3). From a Gaussian fit of the K-continuum visibilities (baselines 28-89 m), we obtained a FWHM diameter of 4.0 ± 0.2 mas.

The AMBER visibilities are in good agreement with the radiative transfer model predictions from Hillier et al. (2001; Figs. 4 & 5). If we fit Hillier et al. model visibilities to the observed AMBER emission line visibilities, we obtain 50% encircled-energy diameters of 4.3, 6.5, and 9.6 mas in the K-band continuum, He I, and the Br γ emission lines, respectively.

In the K-band continuum, we found an elongation toward position angle 128 ± 15° with a projected axis ratio of 1.21 ± 0.08 (2-D visibility fit). This result confirms the earlier finding of van Boeckel et al. (2003) and supports theoretical studies which predict an enhanced mass loss in polar direction for massive stars rotating close to their critical rotation rate (e.g., Dwarkadas & Owocki 2002).

For both the Br γ and He I emission lines, we measured non-zero differential and closure phases within the lines (Fig. 2), indicating a complex, asymmetric object structure. We developed a physically motivated model which shows that the asymmetries measured within the line wings are consistent with the geometry expected for an aspherical, latitude-dependent stellar wind (Weigelt et al. 2006).